Proc. International Conference on Mechanical, Automotive and Mechatronics Engineering (ICMAME 2023)
29-30 April 2023, Dubai, UAE

Optimized Fuzzy MRAS-based Sensorless control of Electric Vehicle Powertrain

Zakaria SEBBOUA
Electrical and Industrial system Laboratory (LSEI)
University of science and technology Houari Boumediene (USTHB)
Algiers, Algeria
zsebboua@usthb.dz

Kenza BOUHOUNE
Electrical and Industrial system Laboratory (LSEI)
University of science and technology Houari Boumediene (USTHB)
Algiers, Algeria
kbouhoune@usthb.dz

Krim YAZID
Electrical and Industrial system Laboratory (LSEI)
University of science and technology Houari Boumediene (USTHB)
Algiers, Algeria
kyazid@usthb.dz

***Abstract*— The paper investigates the performances of speed sensorless indirect field-oriented control of two induction motors used to propel an electric vehicle. The powertrain model, which includes induction motor, electronic differential and vehicle models, is first presented, then an adaptation mechanism based on fuzzy logic controller is designed and optimized by genetic algorithms to ensure the optimal operation of the model reference adaptive system speed estimator. The simulations performed with MATLAB/Simulink software show satisfactory performances of the FuzzyMRAS speed sensorless control over different road conditions.**

Keywords*— *Sensorless control; Electric vehicle (EV); Model reference adaptive system (MRAS); Genetic algorithms (GA); Fuzzy logic controller (FLC); Induction motor (IM).

I. INTRODUCTION

Transportation and mobility play an important role in socio-economic development and business around the world and form a large part of operation in cities [1]. The transport sector has significantly relied on internal combustion engines which consume fuel fossil and emit harmful gases such as carbon dioxide gas [1,2]. Therefore, combustion vehicles contribute to air pollution, global warming and the energy crisis [3]. Furthermore, the combustion engine's energy efficiency is poor. At the present, Vehicle electrification is seen as the main solution to overcome the energy and environment related issues caused by the transport sector. Researchers are expecting to develop energy-efficient, emission-free, and high-performance electric powertrains [3].

The development of electric vehicles has led to the use of various electric machines to electrify the powertrains. The induction machine, is one of the promising traction machines available in the market because of its low cost and high reliability [4,5]. In order to meet the speed and torque requirement intended for use in automotive applications, the IM control strategy is also important as the motor itself. However, optimization of the control strategy is even an essential aspect enabling high performance drive.

Sensorless control drives offer significant advantages in terms of efficiency improvement by avoiding the need for expensive, low-reliability and large sensors. Thus, they contribute to increase the system's reliability by simplifying system's hardware and reducing its size and cost. Hence, sensorless control is recommended for hostile environment applications such as electric vehicle.

Several speed-sensorless induction motor techniques have been proposed in the literature in recent years. These techniques are classified into two classes [6,7] : (i) signal-injection based techniques and, (ii) IM model-based techniques. The last category include Model Reference Adaptive System (MRAS) [10-12], adaptive observer [13], extended Kalman filter [8] and sliding mode observer [9]. In sensorless drives control, MRAS approach is one of the most used technique due to its simplicity and low computational complexity compared to the other techniques.

The paper proposes an optimized fuzzy logic controller (FLC) for speed sensorless control of an electric vehicle propelled by two induction motors with Indirect Rotor Flux Oriented Control (IRFOC) strategy. The optimized FLC is used as adaptation mechanism in rotor flux-based MRAS estimator. In order to achieve the best performances of proposed FuzzyMRAS estimator, FLC gains are optimized using genetic algorithms. The Proposed control is verified using MATLAB/Simulink with different road conditions.

II. ELECTRIC VEHICLE POWERTRAIN MODEL

A. *Induction motor dynamic model*

The state space representation of the induction motor in synchronous rotating frame is given as follows:

$$\begin{aligned} \dot{x} &= Ax + Bu \\ y &= Cx \end{aligned} \tag{1}$$

with:

$$A = \begin{bmatrix} -\frac{1}{\sigma L_s}\left(R_s + \frac{L_m^2}{L_r T_r}\right) & \omega_s & \frac{L_m}{\sigma L_s L_r T_r} & \frac{L_m}{\sigma L_s L_r}\omega_r \\ -\omega_s & -\frac{1}{\sigma L_s}\left(R_s + \frac{L_m^2}{L_r T_r}\right) & -\frac{L_m}{\sigma L_s L_r}\omega_r & \frac{L_m}{\sigma L_s L_r T_r} \\ \frac{L_m}{T_r} & 0 & -\frac{1}{T_r} & \omega_s - \omega_r \\ 0 & \frac{L_m}{T_r} & -(\omega_s - \omega_r) & -\frac{1}{T_r} \end{bmatrix}$$

$$B=\begin{bmatrix}\frac{1}{\sigma L_s} & 0\\ 0 & \frac{1}{\sigma L_s}\\ 0 & 0\\ 0 & 0\end{bmatrix} \quad C=\begin{bmatrix}1&0&0&0\\0&1&0&0\end{bmatrix} \quad x=\begin{bmatrix}i_{ds}\\ i_{qs}\\ \varphi_{dr}\\ \varphi_{qr}\end{bmatrix} \quad u=\begin{bmatrix}v_{ds}\\ v_{qs}\\ 0\\ 0\end{bmatrix} \quad y=\begin{bmatrix}i_{ds}\\ i_{qs}\end{bmatrix}$$

mechanical model:

$$J\frac{d\Omega_r}{dt}=T_{em}-k_f\Omega-T_L \tag{2}$$

with:

$$T_{em}=p\frac{L_m}{L_r}\left(\varphi_{dr}i_{qs}-\varphi_{qr}i_{ds}\right) \tag{3}$$

B. Indirect field oriented control

Rotor field-oriented control is realized by aligning rotor flux with the d-axis as follows:

$$\begin{cases}\varphi_{dr}=\varphi_r\\ \varphi_{qr}=0\end{cases} \tag{4}$$

From motor torque and rotor flux references, the rotor FOC equations are derived based on IM model (1) as follows:

$$I_{qs}=\frac{L_rT_{em}^*}{pL_m\varphi_r^*} \tag{5}$$

$$I_{qs}=\frac{1}{L_m}(T_r\frac{d\varphi_r^*}{dt}+\varphi_r^*) \tag{6}$$

$$V_{ds}=R_sI_{ds}+\sigma L_s\frac{dI_{ds}}{dt}+\frac{L_m}{L_r}\frac{d\varphi_r^*}{dt}-\omega_s\sigma L_sI_{qs} \tag{7}$$

$$V_{qs}=R_sI_{qs}+\sigma L_s\frac{dI_{qs}}{dt}+\omega_s\frac{L_m}{L_r}\varphi_r^*+\omega_s\sigma L_sI_{ds} \tag{8}$$

The motor torque and rotor flux references are the outputs of speed controller and flux weakening bloc (9), respectively [14].

$$\varphi^*=\begin{cases}\varphi^* & if \quad |\Omega_r|\le\Omega_{rn}\\ \varphi^*.\frac{\Omega_{rn}}{\Omega_r} & if \quad |\Omega_r|>\Omega_{rn}\end{cases} \tag{9}$$

The control variables are given by :

$$V_{ds}^*=V_{ds1}^*+\frac{L_m}{L_r}\frac{d\varphi_r^*}{dt}-\omega_s\sigma L_sI_{qs} \tag{10}$$

$$V_{qs}^*=V_{qs1}^*+\omega_s\frac{L_m}{L_r}\varphi_r^*+\omega_s\sigma L_sI_{ds} \tag{11}$$

$$\omega_s=\omega_r+\frac{L_m}{T_r\varphi_r^*}I_{ds} \tag{12}$$

with :

$$V_{ds1}^*=R_sI_{ds}+\sigma L_s\frac{dI_{ds}}{dt} \tag{13}$$

$$V_{qs1}^*=R_sI_{qs}+\sigma L_s\frac{dI_{qs}}{dt} \tag{14}$$

V_{ds1}^* and V_{qs1}^* are obtained through two PI current controllers.

C. Vehicle dynamic model

The vehicle model is deduced from the longitudinal dynamic. The total resistive force F_{res} applied to the vehicle is the sum of the grad (gravitational force) F_{grad}, rolling resistive force F_{roll} and the aerodynamic drag F_{aero} [15].

$$F_{res}=F_{aero}+F_{roll}+F_{grad} \tag{15}$$

with

$$F_{Aero}=\frac{1}{2}\rho C_dA_fv^2 \tag{16}$$

$$F_{roll}=C_{rr}Mg\cos(\alpha) \tag{17}$$

$$F_{grad}=Mg\sin(\alpha) \tag{18}$$

With, α the slop angle and v the linear vehicle's speed in m/s.

Therefore, the motor torque required for traction, in two wheels independent drive case, is given by:

$$T_m=\frac{1}{2}\frac{F_{res}r_w}{\eta_gG} \tag{19}$$

The parameters are described in APPENDIX

D. Electronic differential model

When the vehicle has a banked curve (when cornering), the inner wheels travel lower distance than the outer wheels [16]. Hence, The inner and the outer wheels should be driven at different speeds to prevent vehicle from slipping. An electronic differential is used to adapt the two wheels' speeds to the road conditions so that the inner wheels are slower than the outer ones. The turning movement is described by a simplified model as shown in Fig. 1 [17] . The relationships between the wheels' linear speeds, the turning radius and the vehicle angular speed are given by :

$$v_{out}=\Omega_V(R+\frac{d}{2}) \tag{20}$$

$$v_{in}=\Omega_V(R-\frac{d}{2}) \tag{21}$$

The radius of the curve is expressed as a function of wheelbase and steering angle as:

$$R=\frac{L}{\tan(\delta)} \tag{22}$$

the angular speeds of the two wheels are obtained by Substituting (22) in equations (20) and (21), :

$$(\Omega_w)_{out}=\Omega_V\frac{L+\frac{1}{2}d\tan(\delta)}{L} \tag{23}$$

$$(\Omega_w)_{in}=\Omega_V\frac{L-\frac{1}{2}d\tan(\delta)}{L} \tag{24}$$

The expression of the difference between the two wheels' angular speeds is given by:

$$\Delta\Omega=(\Omega_w)_{out}-(\Omega_w)_{in}=\frac{d\tan(\delta)}{L}\Omega_V \tag{25}$$

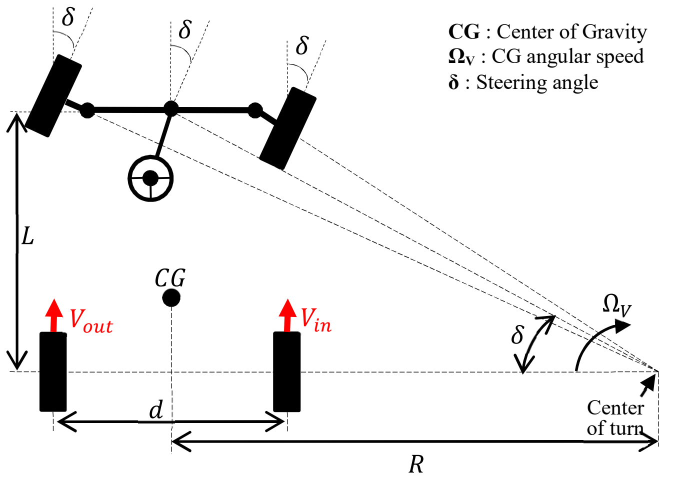

Fig. 1. Turning model

$$\begin{aligned} \delta > 0 &\Rightarrow \quad Turn \quad right \\ \delta = 0 &\Rightarrow \quad Straight \quad ahead \\ \delta < 0 &\Rightarrow \quad Turn \quad left \end{aligned}$$

The speed references for the inner and outer wheels are described as follows:

$$(\Omega_w)_{in}^* = \Omega_V^* - \frac{\Delta\Omega}{2} \qquad (26)$$

$$(\Omega_w)_{out}^* = \Omega_V^* + \frac{\Delta\Omega}{2} \qquad (27)$$

From $(\Omega_w)_{in}^*$ and $(\Omega_w)_{out}^*$, two speed controllers are used to produce two independent torques to drive the inner and outer wheels.

III. PROPOSED SENSORLESS CONTROL

The proposed sensorless control's bloc diagram is presented in Fig. 6. To estimate the speed by the MRAS approach, two models are used. the reference model which does not include the estimated speed and the adaptive model which involve the estimated speed. The two models' outputs are compared and used to estimate the quantity through an adaptation mechanism (Eq.30 in the classic MRAS) that ensures the stability of the controlled system [11].

A. Classic model reference adaptive system

The speed estimation through the classical MRAS requires the estimation of the rotor flux space vector [10]. The reference and adaptive models are given by:

Reference model:

$$\begin{cases} \dfrac{d}{dt}\varphi_{\alpha r} = \dfrac{L_r}{L_m}(v_{\alpha s} - R_s i_{\alpha s} - \sigma L_s \dfrac{d}{dt} i_{\alpha s}) \\ \dfrac{d}{dt}\varphi_{\beta r} = \dfrac{L_r}{L_m}(v_{\beta s} - R_s i_{\beta s} - \sigma L_s \dfrac{d}{dt} i_{\beta s}) \end{cases} \qquad (28)$$

Adaptive model:

$$\begin{cases} \dfrac{d}{dt}\hat{\varphi}_{\alpha r} = \dfrac{L_m}{T_r} i_{\alpha s} - \dfrac{1}{T_r}\hat{\varphi}_{\alpha r} - \omega_r \hat{\varphi}_{\beta r} \\ \dfrac{d}{dt}\hat{\varphi}_{\beta r} = \dfrac{L_m}{T_r} i_{\beta s} - \dfrac{1}{T_r}\hat{\varphi}_{\beta r} - \omega_r \hat{\varphi}_{\alpha r} \end{cases} \qquad (29)$$

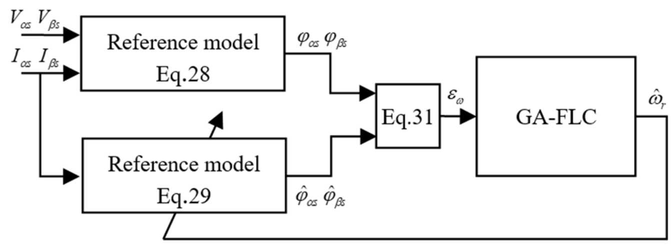

Fig. 2. Bloc diagram of proposed GA-FLC MRAS

Adaptation mechanism:

$$\hat{\omega}_r = (K_p + \frac{K_i}{s})\varepsilon_\omega \qquad (30)$$

with :

$$\varepsilon_\omega = \hat{\varphi}_{\alpha r}\varphi_{\beta r} - \hat{\varphi}_{\beta r}\varphi_{\alpha r} \qquad (31)$$

B. Fuzzy logic controller based MRAS with genetic algorithms optimization

Fig. 2. presents the structure of the proposed GA-Fuzzy MRAS approach, where, an adaptation mechanism is designed based on a Mamdani type fuzzy logic controller in MRAS speed estimator. The FLC has two inputs, which are the speed tunning signal and the change in the speed tunning signal, and one output.

The change in speed tuning signal is expressed as:

$$\Delta\varepsilon_\omega(k) = \varepsilon_\omega(k) - \varepsilon_\omega(k-1) \qquad (32)$$

The estimated rotor speed can be given by:

$$\hat{\omega}_r(k) = \Delta\hat{\omega}_r(k) + \hat{\omega}_r(k-1) \qquad (33)$$

Both output and input signals are multiplied by scaling factors (gains) to adapt the domain of the variable definition [18]. The proposed FLC is presented in Fig. 3.

The output and input variables are divided into seven sets $\{NB, NM, NS, ZE, PS, PM, PB\}$, and each set is represented by a membership function as presented in Fig. 4. Table 1 shows the 49 used fuzzy rules.

The choice of gains coefficients has a huge influence on the FLC performance. Usually, these coefficients are tuned by the trial and error method. Therefore, it is difficult to guarantee optimal performance. In the proposed method, the gains are optimized via genetic algorithms [19] which minimize the cost function (34) according to the optimization procedure presented in Fig. 5.

$$Cost = \int \varepsilon_\omega^2 dt \qquad (34)$$

IV. SIMULATION RESULTS

MATLAB/Simulink software is used to perform the simulations. The optimized FLC rotor flux-based MRAS speed estimator is simulated for two induction motor drives used to propel two wheels of the electric vehicle. Fig. 6 depicts the proposed sensorless control. Different phases (Fig. 7 and Table 2) have been considered to investigate the proposed FuzzyMRAS sensorless control. The results of simulation are depicted in Fig. 8, and the simulation parameters are provided in Table 3.

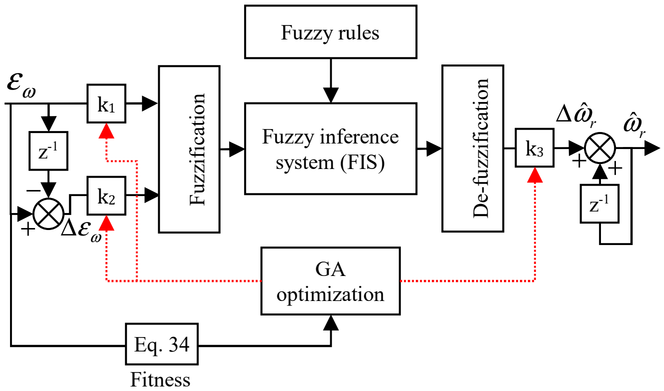

Fig. 3. Optimized GA - FLC structure

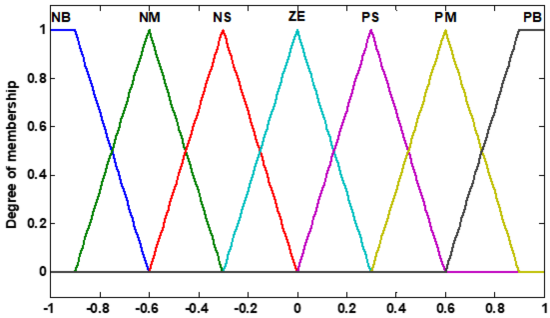

(ZE): ZERO ;(PS): Positive Small; (PM): Positive Medium; (PB); Positive Big; (NB): Negative Big; (NM): Negative Medium; (NS): Negative Small.

Fig. 4. Membership functions of inputs/output

Table I . Inference table

Change in error $\Delta\varepsilon_\omega$	Error ε_ω: NB	NM	NS	ZE	PS	PM	PB
NB	NB	NB	NB	NB	NM	NS	ZE
NM	NB	NB	NB	NM	NS	ZE	PS
NS	NB	NB	NM	NS	ZE	PS	PM
ZE	NB	NM	NS	ZE	PS	PM	PB
PS	NM	NS	ZE	PS	PM	PB	PB
PM	NS	ZE	PS	PM	PB	PB	PB
PB	ZE	PS	PM	PB	PB	PB	PB

The simulation results show that the FuzzyMRAS estimator is able to track the speed accurately in different phases. Good references tracking and robustness to load variation are noticed. The decoupling is maintained.

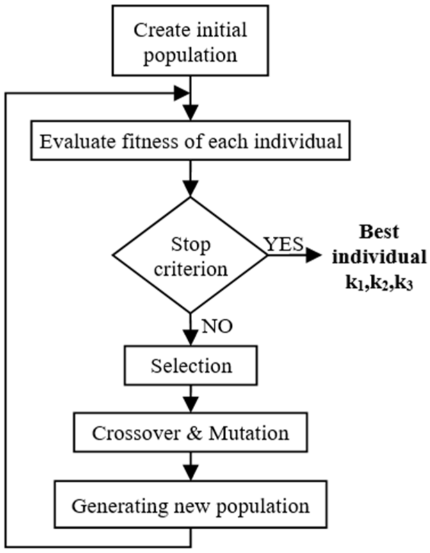

Fig. 5. Genetic algorithms flowchart

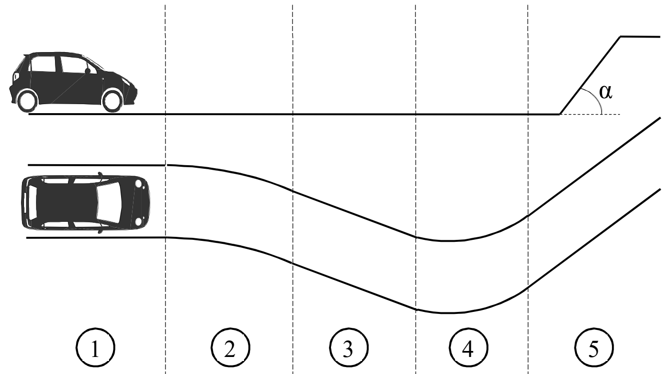

Fig 7. Driving phases

Table II. Driving phases parameters

Phase	Time (s)	Vehicle speed (km/h)
1 Starting	0-15	0:80
2 Curved road ($\delta = 10^o$)	15-30	80
3 Deceleration	30-45	80:60
4 Curved road ($\delta = -15^o$)	45-60	60
5 Climbing a slope ($\alpha = 10^o$)	60-80	60

Table III. Simulation parameters

37 kW Induction motor parametrs					
$\mathbf{N_n}$	1480 rpm	$\mathbf{R_r}$	0.0658 Ω	$\mathbf{L_m}$	0.0291 H
p	2	$\mathbf{L_s}$	0.0314 H	$\mathbf{K_f}$	0.02791 Nm.s/rad
$\mathbf{R_s}$	0.0851 Ω	$\mathbf{L_r}$	0.0291 H	**J**	0.37 kg.m^2
Vehicle parameters					
M: totale mass	1540 kg	**G** : gear ratio		6	
L : wheelbased	2.5 m	$\mathbf{C_{rr}}$: rolling friction coef.		0.0015	
d : vehicle width	1.5 m	$\mathbf{C_d}$: aerodynamic drag coef.		0.2	
$\mathbf{A_f}$: frontal area	1.8 m^2	**ρ**: air dencity		1.225 kg/m^3	
$\mathbf{r_w}$: wheel radius	0.3 m	**g** : gravity acceleration		9.81 m/s^2	
Fuzzy logic controller gains optimized by GA					
$\mathbf{k_1}$		$\mathbf{k_2}$		$\mathbf{k_3}$	
28.186		9.082		33.869	

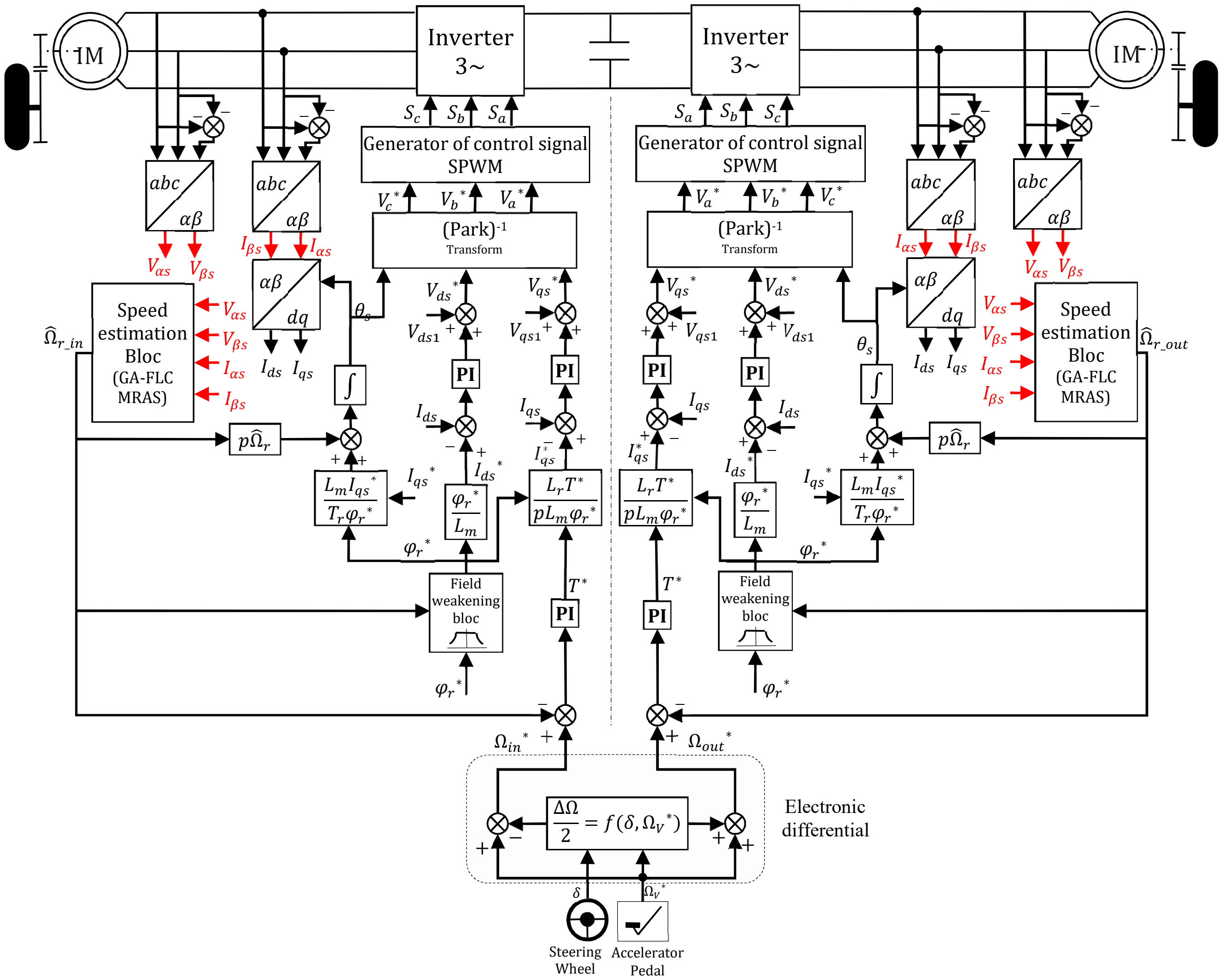

Fig. 6. Bloc diagram of the FuzzyMRAS speed estimation with IRFOC IM drive for electric powertrain

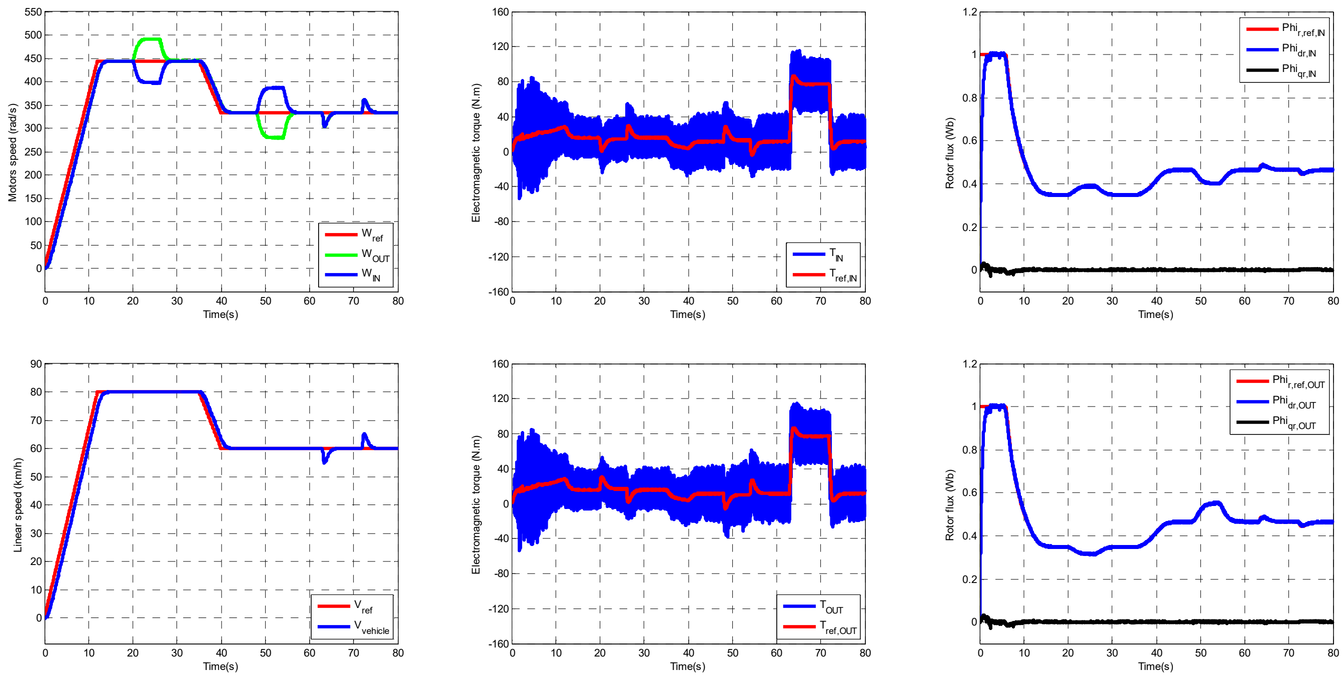

Fig. 7. Simulation results show motor and vehicle speeds, electromagnetic torques and rotor flux

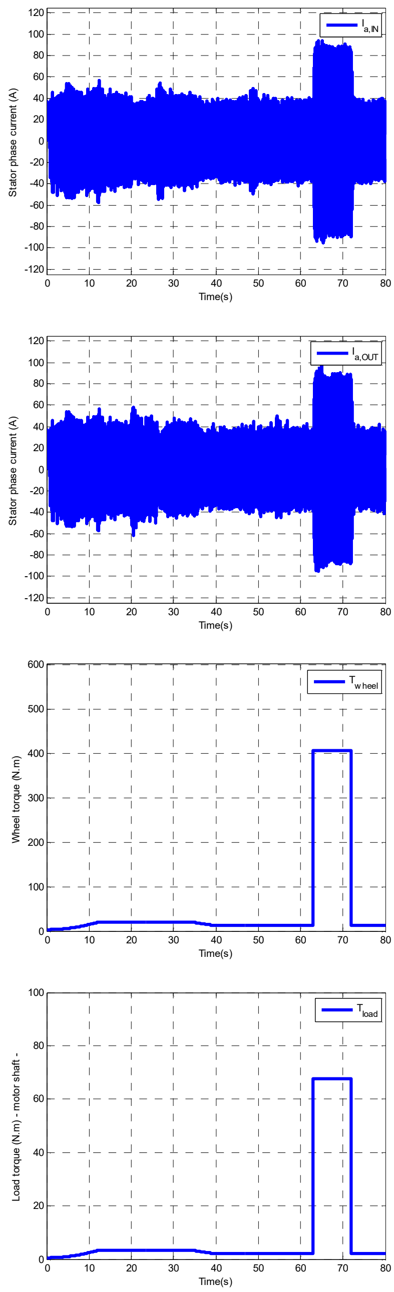

Fig. 8. Simulation results show stator currents, wheel torque and load torque - motor shaft

V. Conclusion

This work addressed speed sensorless electric powertrain control. The powertrain's two rear wheels are driven by two independent induction motors controlled by indirect rotor flux-oriented strategy. The proposed control is based on an FLC-MRAS technique. A fuzzy logic controller has been designed and optimized using genetic algorithms to be used as an adaptation mechanism in the rotor flux-based model reference adaptive system speed estimator. The speed sensorless control based on FuzzyMRAS has been simulated under different road conditions such as acceleration, slope climbing and curved road. Simulation results have shown satisfactory performances of sensorless control using the proposed optimized fuzzy logic controller based-GA, revealing its interest in traction motor drives, in particular EVs.

Acknowledgment

This research is supported by the national research project, under the A01L07UN160420230008code.

References

[1] M. L. De Klerk and A. K. Saha, "A Comprehensive Review of Advanced Traction Motor Control Techniques Suitable for Electric Vehicle Applications," *IEEE Access*, vol. 9, pp. 125080–125108, 2021.

[2] Z. Li, A. Khajepour, and J. Song, "A comprehensive review of the key technologies for pure electric vehicles," *Energy*, vol. 182, pp. 824–839, Sep. 2019.

[3] S. J. Rind, Y. Ren, Y. Hu, J. Wang, and L. Jiang, "Configurations and control of traction motors for electric vehicles: A review," *Chin. J. Electr. Eng.*, vol. 3, no. 3, pp. 1–17, Dec. 2017.

[4] X. Men, Y. Guo, G. Wu, S. Chen, and C. Shi, "Implementation of an Improved Motor Control for Electric Vehicles," *Energies*, vol. 15, no. 13, p. 4833, Jul. 2022.

[5] S. M. N. Ali *et al.*, "Robust Sensorless Control Against Thermally Degraded Speed Performance in an IM Drive Based Electric Vehicle," *IEEE Trans. Energy Convers.*, vol. 35, no. 2, pp. 896–907, Jun. 2020.

[6] D. Xu, B. Wang, G. Zhang, G. Wang, and Y. Yu, "A review of sensorless control methods for AC motor drives," *CES Trans. Electr. Mach. Syst.*, vol. 2, no. 1, pp. 104–115, Mar. 2018.

[7] R. Kumar, S. Das, P. Syam, and A. K. Chattopadhyay, "Review on model reference adaptive system for sensorless vector control of induction motor drives," *IET Electr. Power Appl.*, vol. 9, no. 7, pp. 496–511, Aug. 2015.

[8] Murat Barut, S. Bogosyan, and M. Gokasan, "Speed-Sensorless Estimation for Induction Motors Using Extended Kalman Filters," *IEEE Trans. Ind. Electron.*, vol. 54, no. 1, pp. 272–280, Feb. 2007.

[9] M. Ghanes and Gang Zheng, "On Sensorless Induction Motor Drives: Sliding-Mode Observer and Output Feedback Controller," *IEEE Trans. Ind. Electron.*, vol. 56, no. 9, pp. 3404–3413, Sep. 2009.

[10] C. Schauder, "Adaptive speed identification for vector control of induction motors without rotational transducers," *IEEE Trans. Ind. Appl.*, vol. 28, no. 5, pp. 1054–1061, Oct. 1992.

[11] I. Benlaloui, S. Drid, L. Chrifi-Alaoui, and M. Ouriagli, "Implementation of a New MRAS Speed Sensorless Vector Control of Induction Machine," *IEEE Trans. Energy Convers.*, vol. 30, no. 2, pp. 588–595, Jun. 2015.

[12] A. V. Ravi Teja, V. Verma, and C. Chakraborty, "A New Formulation of Reactive-Power-Based Model Reference Adaptive System for Sensorless Induction Motor Drive," *IEEE Trans. Ind. Electron.*, vol. 62, no. 11, pp. 6797–6808, Nov. 2015.

[13] W. Sun, J. Gao, Y. Yu, G. Wang, and D. Xu, "Robustness Improvement of Speed Estimation in Speed-Sensorless Induction Motor Drives," *IEEE Trans. Ind. Appl.*, vol. 52, no. 3, pp. 2525–2536, May 2016.

[14] K. Bouhoune, K. Yazid, M. S. Boucherit, B. Nahid-Mobarakeh, and M. Menaa, "Electrical-Sensorless Control of Induction Motor," in *2019 IEEE 10th International Symposium on Sensorless Control for Electrical Drives (SLED)*, Turin, Italy, Sep. 2019, pp. 1–6.

[15] M. Jafari, A. Gauchia, K. Zhang, and L. Gauchia, "Simulation and Analysis of the Effect of Real-World Driving Styles in an EV Battery Performance and Aging," *IEEE Trans. Transp. Electrification*, vol. 1, no. 4, pp. 391–401, Dec. 2015.

[16] J. L. F. Daya, P. Sanjeevikumar, F. Blaabjerg, P. W. Wheeler, and J. O. Ojo, "Implementation of Wavelet-Based Robust Differential Control for Electric Vehicle Application," *IEEE Trans. Power Electron.*, vol. 30, no. 12, pp. 6510–6513, Dec. 2015.

[17] A. Draou, "Electronic Differential Speed Control for Two in-wheels Motors Drive Vehicle," p. 6, 2013.

[18] K. Bouhoune, K. Yazid, M. S. Boucherit, and A. Chériti, "Hybrid control of the three phase induction machine using artificial neural networks and fuzzy logic," *Appl. Soft Comput.*, vol. 55, pp. 289–301, Jun. 2017.

[19] M. Chebre, A. Meroufel, and Y. Bendaha, "Speed Control of Induction Motor Using Genetic Algorithm-based PI Controller," *Acta Polytech. Hung.*, vol. 8, no. 6, p. 13, 2011.